Efficient Calculation of Isotropic Hyperfine Constants of Phosphorus Radicals Using Density Functional Theory

Minh Tho Nguyen,* Steven Creve, and Luc G. Vanquickenborne

Department of Chemistry, University of Leuven, Celestijnenlaan 200F, B-3001 Leuven, Belgium

Received: November 27, 1996; In Final Form: February 21, 1997[⊗]

Calculations of the isotropic hyperfine coupling constants of phosphorus nuclei in different environments have been carried out using density functional theory with both B3LYP and B3PW91 functionals and a variety of one-electron basis sets. A set of 35 radicals, radical cations, and triplet species containing P have been analyzed, including the set recently examined by Cramer and Lim (*J. Phys. Chem.* **1994**, *98*, 5024) using the UMP2 method. The dependency of the calculated spin densities with respect to the methods, basis sets, and geometries have been investigated. Overall, the B3LYP method, in conjunction with a TZVP basis optimized for DFT calculations and further augmented by tight 1s-functions on all heavy atoms, appears to be the most efficient treatment, presumably owing to better cancelations of intrinsic errors. Depending on the size of the species examined and/or the spin contamination of UHF references, use of UMP2 geometries is preferred, otherwise B3LYP/6-311G(d,p) geometries are a reasonable choice. In both cases, linear correlation between computed and observed values have been found with slopes close to unity and small intercepts $\leq$10 G.

Introduction

The importance of radicals as intermediates and precursors in chemical reactions is well-known. However, due to their short lifetimes and high reactivities, it is often very difficult to detect and characterize them experimentally. One of the popular spectroscopic methods used to obtain information on these species is the electron spin resonance (ESR) technique. The most interesting properties usually gained from such experiments are the hyperfine coupling constants (hfcc's) related to certain nuclei in the radical. Major applications of ESR are the identification and structural characterization of chemical species having unpaired electrons. Thus, theoretical predictions become more valuable as molecular geometries and hyperfine coupling constants can be calculated and thereby furnishing an important additional source of information. Consequently, it is not surprising that the calculation of hyperfine properties has received a great deal of attention of theoretical chemists.

The most important coupling constant is the isotropic parameter. Unfortunately, this property turns out to be difficult to obtain with great accuracy by use of quantum-chemical methods, as it is strongly sensitive not only to the quality of the calculation, such as electron correlation and the basis set used, but also to the molecular geometry. Traditional ab initio molecular orbital theory calculations require massively correlated wave functions (e.g., multireference configuration interaction (MRCI), quadratic configuration interaction (QCI), and coupled cluster (CC) techniques) as well as very large basis sets to achieve quantitative agreement with experiment. Needless to say, such requirements tend to prohibit useful predictions on large chemical systems. Therefore, much effort has been directed at the search for economic but reliable methods in computing the spin properties. In this regard, Cramer and Lim[1] have recently analyzed the performance of some relatively simple MO methods including the unrestricted Hartree−Fock (UHF) and its spin-projected version (PUHF) as well as second-order perturbation theory (UMP2). As test cases, a set of 25 radicals containing phosphorus atoms have been considered. Upon a detailed systematic comparison of computed values obtained by changing the method, basis set, and geometry, with available experimental data, these authors[1] arrived at the conclusion that the UMP2 method, in conjunction with the split-valence plus polarization 6-311G(d,p) basis set and based on UHF/6-31G(d,p) optimized geometries (instead of UMP2/6-31G(d,p) geometries), provides the best correlation with experiment, the rms error being 36.1 G.[1] These results[1] emphasize again the primordial importance of the geometry employed. The fact that less accurate UHF geometries yield better isotropic hfcc's than the, in principle, more accurate UMP2 geometries, points strongly toward an inherent cancelation of errors, either experimental or theoretical. In fact, as many ESR experiments were carried out in inert matrices, a certain small but significant geometrical distortion from gas phase structures could not be ruled out.

Note that the UHF wave functions for the set of 25 doublet radicals considered are not particularly contaminated by higher-spin states; the expectation values $\langle S^2 \rangle$ ranging from 0.76 to 0.81. It is well-known that, when the spin contamination of UHF references becomes large, an UMP2 treatment of the energies or spin properties is no longer valid, due to a slow convergence of the perturbation expansion. As a consequence, an intrinsic shortcoming of the approach suggested by Cramer and Lim[1] is that it cannot be generalized; its application remains mandatorily dependent on the degree of spin contamination suffered by the UHF wave functions under consideration.

In recent years, the increasing popularity of density functional methods (DFT)—due to its partial incorporation of correlation effects at the mere cost of self-consistent field (SCF) calculations—has also a beneficial impact on hfcc's calculations. One of the characteristics of DFT is that, in the framework of unrestricted formalism, the spin contamination is no longer an important or relevant parameter. A number of groups[3,4] has demonstrated independently that DFT may yield good theoretical values for spin properties. Recently, Cramer and Lim also investigated the performance of various density functionals using the same set of 25 radicals.[2] It turned out that DFT hfcc calculations yield similar results as MP2//MP2 calculations. However, the obtained accuracy is considerably less than that obtained for MP2//UHF calculations. Cramer and Lim also

[⊗] Abstract published in *Advance ACS Abstracts,* April 1, 1997.

S1089-5639(96)03936-9 CCC: $14.00

noticed that, in general, DFT yields best performance using MP2 geometries, followed by UHF and DFT geometries. In the appropriate sections of this paper, reference and comparison will be made to the results obtained by these authors.

In a previous work,[5] we have assessed the performance of different high level ab initio MO and DFT methods and found that the B3LYP functional[6,7,12] computes relatively accurate hfcc's of phosphorus-containing radicals. A purposely tailored basis set, which yields satisfactory results for a small test set of eight radicals having doublet and triplet electronic states, was introduced. In the present work, an attempt is made to extend this test to a larger set of 35 phosphorus-containing radicals, for which a total of 48 experimental isotropic hfcc's for different nuclei are available. The present list of radicals includes essentially those radicals examined by Cramer and Lim[1,2] in both their MP2 and DFT studies and is extended by a few more radicals and some triplet phosphinidenes. Particular attention is paid to the computed results in what follows. Several chemical aspects, for example, the substituent effects or the changes of spin properties with respect to environments, are not discussed in detail.

Computational Details

The isotropic hyperfine coupling for a nucleus N is obtained from the following expression 1:

$$a_{iso}(N) = (4\pi/3)gg_N\beta\beta_N\langle S_z\rangle^{-1}\rho(N) \quad (1)$$

where g is the electronic g-factor, here set to the free electron value 2.0023; β is the Bohr magneton and g_N and β_N are the analogues for nucleus N. $\rho(N)$ is the Fermi contact integral corresponding to the spin density at nucleus N and is given by (2):

$$\rho(N) = \sum_{\mu\nu} P_{\mu\nu}^{\alpha-\beta}\langle\phi_\mu(r_{kN})|\delta(r_{kN})|\phi_\nu(r_{kN})\rangle \quad (2)$$

where $P_{\mu\nu}^{\alpha-\beta}$ is an element of the one-electron spin denstity matrix and ϕ designates the atomic basis functions. Replacing the constants in formulas 1 and 2 by their appropriate values yields the following conversion factors for the different nuclei in radicals with a doublet electronic state (a_{iso} in G):

$$a_{iso}(^1H) = 1594.9 \times \rho(^1H)$$

$$a_{iso}(^{13}C) = 401.1 \times \rho(^{13}C)$$

$$a_{iso}(^{14}N) = 57.6 \times \rho(^{14}N)$$

$$a_{iso}(^{17}O) = -43.3 \times \rho(^{17}O)$$

$$a_{iso}(^{19}F) = 1501.3 \times \rho(^{19}F)$$

$$a_{iso}(^{31}P) = 646.3 \times \rho(^{31}P)$$

$$a_{iso}(^{33}S) = 40.8 \times \rho(^{33}S)$$

$$a_{iso}(^{35}Cl) = 52.1 \times \rho(^{35}Cl)$$

To obtain the conversion factors for triplet states, the above constants should be divided by a factor of 2.

Geometries of the species considered were optimized using the B3LYP,[6,7,12] B3PW91[6,8,12] and UMP2 methods. Subsequently, single-point DFT calculations were performed at the obtained geometries, using a variety of basis sets. While the 6-311G(d,p) basis set was used for the DFT optimizations, the smaller 6-31G(d,p) set was used for UMP2 optimizations for reasons of computational cost. Throughout the UMP2 calculations, all core electrons were included in the correlation treatment. Concerning the hfcc calculations, the basis sets were chosen in the light of our previous theoretical study on a smaller subset of phosphorus containing radicals.[5] Accordingly, the following basis sets were used: the 6-311G(d,p); a DFT-optimized valence triple-ζ basis, TZVP,[9] and some variants proposed by us in which tight s-functions were added to the core orbitals, namely, TZVP+1s on P only and TZVP+1s on all heavy atoms, the loosely contracted IGLO-III set,[10] and the correlation consistent cc-pVTZ basis.[11] In the discussion and tables given hereafter, we will use the shorthand notations TZVP′ and TZVP″ to designate TZVP+1s on P and TZVP+1s on heavy atoms, respectively. The TZVP basis set,[9] optimized within the framework of the local spin density approach (LSDA), consists of a (311/1) basis for H, a (7111/411/1) basis for first-row elements, and a (73111/6111/1) basis for second-row elements. We have found[5] that further improvements can be obtained by adding a tight s-function to the core s-orbital. In other words, the electronic distribution around the nucleus is somewhat better described upon addition of a tight 1s-orbital. The exponent of the s-function added was optimized with respect to the energy of the atom under consideration. Hence, the following exponents resulted:

C = 51751.2

N = 72117.7

O = 96477.8

F = 121156.0

P = 435485.0

S = 503435.1

Cl = 566442.0

All geometry optimizations and calculations of isotropic hfcc's were performed by the Gaussian 94 suite of electronic structure programs.[12] It should be noted that the effects of vibrational averaging on the calculated hfcc's are ignored in this study.

Results and Discussion

Geometries. Geometries were optimized using both B3LYP and B3PW91 functionals in combination with the 6-311G(d,p) basis set and at the UMP2 level of theory with the 6-31G(d,p) basis. To simplify the presentation of data, a full list of optimized geometrical parameters is not shown here, but is available as Supporting Information. Note that selected UMP2/6-31G(d,p) parameters have been given in ref 1 for the set of 25 radicals. While both B3LYP and B3PW91 geometries are very similar to each other, the UMP2-derived geometries are expected to be closer to experimental values, as we noted in our previous study on phosphorus-containing radicals.[5] This is also observed in a recent paper,[13] that pointed out that, for molecules containing second-row elements, while B3LYP yields bond lengths significantly too long, UMP2 results compare more favorably to the experimental. A short summary of differences in geometry is made in Table 1. The deviations of B3LYP/6-311G(d,p) and B3PW91/6-311G(d,p) geometrical parameters

TABLE 1: Mean Deviations of DFT-Computed Bond Lengths from MP2/6-31G(d,p) Bond Lengths (Å). The Number of Data Considered Is Shown in Parentheses

	6-311G(d,p)	
	B3LYP	B3PW91
P−H (14)	0.024	0.025
P−C (3)	0.010	0.000
P−O (15)	−0.010	−0.014
P−S (8)	0.027	0.010
P−F (11)	0.013	0.007
P−Cl (10)	0.058	0.032

TABLE 2: Electronic States and Total Energies of the Species Considered

radical	radical no.	state	MP2,[a] 6-31G(d,p)
PH_3^+	**1**	$^2A_1$	−342.249 47
$P(CH_3)_3^+$	**2**	$^2A_1$	−459.896 22
PCl_3^+	**3**	$^2A_1$	−1719.393 59
PF_3^+	**4**	$^2A_1$	−639.371 42
$P_2H_6^+$	**5**	^2B_u	−684.882 74
H_2POH^+	**6**	$^2A'$	−417.317 05
H_2PO	**7**	$^2A'$	−417.004 55
H_2PS	**8**	$^2A'$	−739.620 71
Me_2PO	**9**	$^2A'$	−495.413 60
PH_2	**10**	$^2B_1$	−341.964 61
PF_2	**11**	$^2B_1$	−540.072 57
PCl_2	**12**	$^2B_1$	−1260.078 43
PH_4	**13**	$^2A_1$	−343.088 80
PF_4	**14**	$^2A_1$	−739.351 78
PCl_4	**15**	$^2A_1$	−2179.327 13
H_3PF	**16**	$^2A'$	−442.151 83
HPF_3	**17**	$^2A'$	−640.283 19
PF_5^-	**18**	$^2A_1$	−839.060 26
PCl_5^-	**19**	$^2A_1$	−2639.052 80
PO_4^{2-}	**20**	$^2B_2$	−640.915 23
$PO_2S_2^{2-}$	**21**	$^2B_2$	−1286.196 24
POS_3^{2-}	**22**	$^2A''$	−1608.799 19
PS_4^{2-}	**23**	$^2B_2$	−1931.420 46
H_2PO_2	**24**	$^2B_2$	−492.025 25
H_2PO_4	**25**	$^2B_1$	−642.213 83
PO_2Cl_2	**26**	$^2B_2$	−1410.127 34
$POCl_3^-$	**27**	$^2A'$	−1794.862 11
$PFSCl_2^-$	**28**	$^2A'$	−1757.452 79
PO_3F^-	**29**	$^2A''$	−665.674 60
PH	**30**	$^3\Sigma^-$	−341.353 24
PCH_3	**31**	$^3A_2$	−380.546 66
PNH_2	**32**	$^3A''$	−396.573 03
PPH_2	**33**	$^3A''$	−682.782 05
POH	**34**	$^3A''$	−416.415 38
PSH	**35**	$^3A''$	−739.016 76

[a] Using the MP2/6-31G(d,p)-optimized geometry.

with respect to UMP2/6-31G(d,p) parameters are shown for different types of bonds. Note that this table deals with mean deviations, i.e., the sign of the deviation is included. It is seen that both B3LYP and B3PW91, in general, overestimate bond lengths with respect to UMP2. Only for P−O bonds is a small underestimation found. P−H bonds are generally too long by about 0.025 Å for both functionals. While P−C and P−F bonds are only slightly overestimated by both functionals, the error is much worse for the heavy atoms: B3LYP overestimates the P−S bonds by 0.027 Å and the P−Cl bonds even by 0.058 Å! In general, it should also be noted that the errors with respect to UMP2 are smaller for B3PW91 than for B3LYP. As mentioned above, this difference in geometry will have a significant influence on computed hyperfine coupling constants.

Isotropic Hyperfine Coupling Constants. Table 2 shows the species under consideration, their electronic states studied, and their total electronic energies calculated at the UMP2/6-31G(d,p) level using optimized geometries. ^{31}P isotropic hfcc's deduced from a selection of methods are displayed in Tables 3 and 4. Only the hfcc's obtained with the TZVP basis sets and the IGLO-III set are shown; the 6-311G(d,p) and cc-pVTZ results are omitted in these tables, but can be obtained from the authors on request. In the following section, results for groups of analogous radicals will be discussed and compared with the results obtained by Cramer and Lim,[1,2] as well as with available experimental data. Subsequently, a statistical analysis of the large number of calculated data will be presented. Detail of the basis set performance will not be discussed as this has been reported in our previous study.[5] We will use shorthand notations for the different computational models employed; namely, B3LYP designates a B3LYP single-point calculation using the corresponding B3LYP/6-311G(d,p) geometry and the same holds for B3PW91. On the other hand, B3LYP//MP2 and B3PW91//MP2 designate B3LYP or B3PW91 single-point calculations using the UMP2/6-31G(d,p) geometry, respectively.

^{31}P Isotropic Hyperfine Coupling Constants. The isotropic ^{31}P hfcc's calculated by four different models (B3LYP, B3PW91, B3LYP//MP2, and B3PW91//MP2) using different basis sets are shown in Tables 3 and 4, which also includes, for the purpose of comparison, the UMP2/6-311G(d,p)//UHF/6-31G-(d,p) values reported in ref 1 (this method will be referred to as UMP2//UHF).

PH_3^+, $P(CH_3)_3^+$, PCl_3^+, PF_3^+, and $P_2H_6^+$. For the PH_3^+ radical cation, all four models predict isotropic hfcc's in fair agreement with the experimental values. The IGLO-III basis yields hfcc's approximately 20 G lower than the TZVP results. While PH_3^+ has not been studied in ref 1, its methylated analogue, $P(CH_3)_3^+$, has. The experimental hyperfine splitting of the latter radical cation is about 23 G lower than that of PH_3^+, which indicates a stronger delocalization of the unpaired electron from P to the methyl groups. While the UMP2//UHF value is in good agreement with experiment, our values are somewhat less, but the qualitative trend is well reestablished. PCl_3^+ shows a much higher coupling constant than PH_3^+ or $P(CH_3)_3^+$. This fact is reasonably well reproduced by all DFT calculations as well as by the UMP2//UHF method. In this case, DFT calculations yield slightly better values than UMP2//UHF, in particular the IGLO-III basis set gives excellent agreement with experiment. It is remarkable that PF_3^+ exhibits a coupling constant which is even higher than that of PCl_3^+. The isotropic hfcc of $P_2H_6^+$, which has not been studied in ref 1, is also reasonably well reproduced by all DFT methods.

PH_2, PF_2, and PCl_2. These three radicals show similar hyperfine splittings. While DFT results for PH_2 and PCl_2 are in good agreement with the experimental, somewhat less accurate values are obtained for PF_2. The UMP2//UHF method predicts a better coupling constant for PF_2 than the four DFT methods, but the reverse happens for PCl_2. For these dicoordinated radicals, use of the IGLO-III basis in combination with DFT seriously underestimates the experimental values. It is interesting to note that, while perfluorination induces an upward shift of the splitting, perchlorination produces a reverse effect.

H_2PO, H_2PS, Me_2PO, and H_2POH^+. Of these four radicals, only Me_2PO has been observed experimentally. The hfcc's of both H_2PO and H_2PS have been estimated in earlier studies.[14,15] While the UMP2//UHF-predicted coupling constant is larger than the experimental splitting by 35 G, our calculations underestimate it by somewhat less than 35 G. For H_2PO, H_2PS, and H_2POH^+, large discrepancies of more than 100 G between the DFT results and UMP2//UHF appear. They are also different from the previous MRCI values.[14,15] Unfortunately, to our knowledge, no experimental results are available. Both methods show, however, the same trend: the isotropic coupling increases following protonation, from H_2PO to its

TABLE 3: ^{31}P Isotropic Hyperfine Coupling Constants (G) As Calculated by DFT Methods, Using DFT Geometries

	B3LYP[a]				B3PW91[b]						
radical	TZVP	TZVP′	TZVP″	IGLO-III	TZVP	TZVP′	TZVP″	IGLO-III	UMP2//UHF[c]	exptl	ref
1[d]	405.4	418.6	418.6	402.0	398.3	412.4	412.4	392.3		419.6	16
2	343.1	354.5	354.5	348.9	344.7	356.2	356.2	348.0	402.3	393.3	17
3	745.0	769.9	769.9	838.5	743.2	768.0	768.0	831.9	767.1	833.5	18
4	1257.0	1299.1	1299.1	1323.6	1252.9	1294.8	1294.8	1303.6			
5	542.2	560.4	560.4	553.9	540.3	558.4	558.4	548.5		590.2	16
6	407.8	421.5	421.5	423.9	403.0	416.4	419.3	416.4	507.2		
7	326.2	337.1	337.1	357.0	317.4	328.1	328.1	344.6	206.8		
8	218.5	225.8	225.8	233.7	219.2	226.5	226.5	235.9	112.8		
9	326.6	337.5	337.5	352.1	320.2	330.9	330.8	343.3	410.4	375.0	17
10	76.7	79.2	79.2	57.4	65.8	67.3	67.3	49.7		77.4	19
11	97.4	100.6	100.6	63.5	90.2	93.2	93.2	54.8	90.1	84.6	20
12	60.1	62.0	62.0	48.1	52.6	54.3	54.3	43.2	45.5	68.0	21
13	499.7	514.0	514.0	560.7	473.4	489.3	489.3	529.0	512.0	519.3	22
14	1315.5	1359.6	1359.5	1387.3	1290.7	1334.0	1334.0	1340.5	1275.0	1330.0	20
15	1291.8	1335.1	1335.1	1404.9	1270.6	1313.3	1313.2	1370.6	1250.1	1233.0	23
16	746.3	771.3	771.3	781.6	721.2	745.4	745.4	747.4	720.1	721.3	24
17	1014.2	1048.2	1048.2	1057.4	995.0	1028.3	1028.3	1024.4	1002.6	1030.8	24
18	1435.1	1483.1	1483.1	1512.2	1383.4	1429.7	1429.7	1442.0	1281.1	1328.2	25
19	1434.5	1482.6	1482.6	1569.3	1465.1	1514.2	1514.2	1588.3	1586.0	1617.0	23
20	−33.7	−34.9	−34.9	−32.7	−35.1	−36.3	−36.3	−33.7	−12.7	−19.2	26
21	−14.6	−15.0	−15.0	−14.0	−15.0	−15.5	−15.5	−13.8	−19.0	−16.8	27
22	−16.0	−16.5	−16.5	−13.7	−16.5	−17.0	−17.0	−13.7	−15.5	−13.5	27
23	−13.2	−13.7	−13.7	−11.1	−14.0	−14.5	−14.5	−11.5	−21.3	−14.7	27
24	−62.4	−64.5	−64.5	−57.5	−64.4	−66.6	−66.6	−58.7	−22.7		
25	−51.1	−52.8	−52.8	−48.5	−53.1	−54.9	−54.9	−49.8	−20.9	−29.0	28
26	−50.9	−52.6	−52.1	−49.5	−51.7	−53.0	−52.6	−52.8	−19.9	−44.3	29
27	1288.1	1331.4	1331.3	1408.8	1332.8	1377.5	1377.5	1445.2	1332.7	1371.0	29
28	1027.1	1061.6	1061.6	1119.7	1038.6	1073.4	1073.4	1122.2	1123.5		
29	−49.2	−50.8	−50.8	−46.6	−51.2	−52.9	−52.9	−47.8	−37.0	−39.1	30
30	54.3	56.0	56.0	25.8	40.3	41.5	41.5	13.3		44.7	31
31	53.3	54.8	54.8	26.8	40.5	41.6	41.6	13.9			
32	52.4	54.1	54.1	24.7	40.1	41.5	41.5	12.9			
33[e]	38.4	39.6	39.6	18.7	27.3	28.0	28.0	10.0			
	8.4	8.4	8.4	5.9	3.9	4.0	4.0	2.8			
34	54.1	55.8	55.8	23.3	41.0	42.3	42.3	10.1			
35	41.3	42.5	42.5	18.9	28.4	29.1	29.1	8.0			

[a] B3LYP calculations using the B3LYP/6-311G(d,p) geometry. [b] B3PW91 calculations using the B3PW91/6-311G(d,p) geometry. [c] UMP2/6-311G(d,p) using UHF/6-31G(d,p) geometries, ref 1. [d] See Table 2 for the radical's formula. [e] The first coupling of PPH_2 refers to the phosphinidene P, the second coupling to the phosphino P.

protonated form H_2POH^+, but instead decreases in going to the sulfur analogue H_2PS.

PH_4, PF_4, PCl_4, H_3PF, and HPF_3. For these radicals containing a tetracoordinated phosphorus atom, experimental data are available. The DFT derived hfcc's are in good agreement with experiment and better than the UMP2//UHF results for both PF_4 and HPF_3. The corresponding values for H_3PF hfcc's are in reasonable agreement with the experimental but they are not as accurate as the value obtained by UMP2//UHF. The PH_4 hyperfine splitting shows a stronger dependency on the geometry used; in this case, the B3LYP model using both TZVP′ and TZVP″ basis sets yields good accuracy. Use of the B3PW91 or UMP2 geometry yields consistently underestimated values. With a certain theoretical model, the IGLO-III basis set systematically overshoots the corresponding TZVP′ and TZVP″ values by about 40 G. The PCl_4 case is particularly interesting. While our DFT calculations provide ^{31}P hfcc's close to 1300 G, the UMP2//UHF value is 1250.1 G, and the experimental value quoted in ref 1 is only 1233 G. However, the experimental paper[23] contains two isotropic ^{31}P hfcc's for this radical: while the coupling of 1233 G was observed in a $[PCl_3]$ system, a coupling of 1310 G was observed in a $[PCl_4-PCl_6^-]$ system. Hence, it is embarassing that the relative performance of a model may depend upon the choice of experimental data!

The experimental values show that the hyperfine coupling of the ^{31}P nucleus increases along with the increasing presence of fluorine atoms: while PH_4 has a hfcc of only 591.3 G, this changes over 721.3, 1030.8, and up to 1330.0 G in the sequence $PH_4 \rightarrow H_3PF \rightarrow HPF_3 \rightarrow PF_4$. The PCl_4 hfcc is similar to that of PF_4. It is thus apparent that halogenation induces consistently an upward shift of the splitting, which is by far larger than that observed in dicoordinated species (see PH_2 and PF_2).

PF_5^- and PCl_5^-. While the DFT-predicted hfcc's of PF_5^- are considerably overestimated (from 4 to 180 G), the UMP2//UHF value is underestimated by 47 G. For PCl_5^- the UMP2//UHF value is better than all TZVP, TZVP′, or TZVP″ calculations, but the IGLO-III basis set in combination with the UMP2 geometry, yields the better results. For both radicals, a large geometry dependence is thus observed, with the UMP2 geometry generally giving better predictions; the bipyramid structure seems not to be well represented by DFT calculations.

PO_4^{2-}, $PO_2S_2^{2-}$, POS_3^{2-} and PS_4^{2-}. This is another series of analogous molecules for which experimental ^{31}P isotropic hfcc's are well established. All ^{31}P hfcc's are negative for these molecules and vary over a very small range (from −19.2 to −13.5 G, experimental values). The absolute deviations from the experimental results of the various models, including the UMP2//UHF method, are very similar. While our DFT values suggest that the hfcc's slightly increase with an increasing number of S atoms, the absolute values of the hfcc's are actually too small to allow any general trend to be identified.

H_2PO_2 and H_2PO_4. While the DFT splittings are smaller than the experimental one of H_2PO_4 by about 20 G, the UMP2//UHF value is in reasonable agreement. For H_2PO_2, where no

TABLE 4: ^{31}P Isotropic Hyperfine Coupling Constants (G) As Calculated by DFT Methods, Using UMP2 Geometries

	B3LYP//MP2[a]				B3PW91//MP2[b]						
radical	TZVP	TZVP′	TZVP″	IGLO-III	TZVP	TZVP′	TZVP″	IGLO-III	UMP2//UHF[c]	exptl	ref
1[d]	397.1	410.3	410.3	392.1	396.2	409.4	409.4	389.4		419.6	16
2	344.0	355.4	355.4	349.6	348.0	359.6	359.6	351.3	402.3	393.3	17
3	747.1	772.1	772.1	838.7	743.8	768.7	768.7	831.3	767.1	833.5	18
4	1262.3	1304.6	1304.6	1329.7	1258.4	1300.5	1300.5	1310.9			
5	540.3	558.4	558.4	551.7	529.0	546.7	546.7	536.5		590.2	16
6	396.4	409.7	409.6	411.6	394.7	407.9	407.9	407.4	507.2		
7	319.0	329.7	329.7	349.9	308.7	319.0	319.0	335.8	206.8		
8	237.6	245.6	245.6	256.5	230.7	238.4	238.4	248.7	112.8		
9	327.6	338.5	338.5	352.9	321.6	332.4	332.4	344.8	410.4	375.0	17
10	77.4	79.9	79.9	58.8	66.7	69.0	69.0	50.8		77.4	19
11	97.3	100.5	100.5	62.5	90.1	93.1	93.1	54.8	90.1	84.6	20
12	63.3	65.3	65.3	51.1	54.4	56.2	56.2	45.1	45.5	68.0	21
13	464.7	480.2	480.2	528.0	444.8	459.7	459.7	500.8	512.0	519.3	22
14	1294.3	1337.7	1337.7	1362.7	1279.3	1322.1	1322.1	1328.0	1275.0	1330.0	20
15	1268.7	1311.2	1311.2	1371.3	1255.6	1297.7	1297.7	1349.1	1250.1	1233.0	23
16	705.1	728.7	728.7	737.4	687.7	710.7	710.7	711.2	720.1	721.3	24
17	987.9	1021.0	1021.0	1028.4	975.0	1007.6	1007.6	1002.7	1002.6	1030.8	24
18	1363.8	1409.5	1409.5	1434.7	1332.3	1376.9	1376.9	1387.3	1281.1	1328.2	25
19[d]	1507.7	1558.3	1558.3	1637.6	1499.3	1549.6	1549.5	1617.6	1586.0	1617.0	23
20	−33.0	−34.1	−34.1	−32.0	−34.6	−35.7	−35.7	−33.2	−12.7	−19.2	26
21	−13.9	−14.4	−14.4	−13.7	−14.7	−15.2	−15.2	−13.9	−19.0	−16.8	27
22	−13.9	−14.3	−14.3	−12.1	−14.6	−15.1	−15.1	−12.3	−15.5	−13.5	27
23	−12.8	−13.3	−13.3	−10.8	−13.8	−14.3	−14.3	−11.4	−21.3	−14.7	27
24	−59.7	−61.7	−61.7	−55.0	−62.2	−64.3	−64.3	−56.6	−22.7		
25	−50.7	−52.4	−52.4	−48.2	−53.2	−54.9	−54.9	−49.8	−20.9	−29.0	28
26	−49.5	−51.2	−51.2	−47.5	−50.7	−52.4	−53.9	−48.0	−19.9	−44.3	29
27	1367.8	1410.5	1415.2	1492.7	1362.3	1408.0	1408.0	1473.8	1332.7	1371.0	29
28	1053.6	1088.9	1088.9	1145.9	1046.6	1081.7	1081.6	1130.1	1123.5		
29	−40.5	−41.9	−41.9	−38.7	−42.3	−43.7	−43.7	−40.1	−37.0	−39.1	30
30	54.6	56.4	56.4	27.2	40.9	42.2	42.2	15.3		44.7	31
31	53.2	54.8	54.8	26.0	40.1	41.2	41.2	13.5			
32	52.4	54.1	54.1	24.7	40.1	41.4	41.4	12.8			
33[e]	39.2	40.3	40.3	19.5	27.6	28.4	28.4	10.3			
	7.8	8.1	8.1	5.7	3.8	3.9	3.9	2.6			
34	55.2	55.8	55.6	22.7	40.6	42.0	42.0	10.1			
35	42.1	43.3	43.3	19.8	28.4	29.4	29.4	8.3			

[a] B3LYP calculations using the UMP2/6-31G(d,p) geometry. [b] B3PW91 calculations using the UMP2/6-31G(d,p) geometry. [c] UMP2/6-311G(d,p) using UHF/6-31G(d,p) geometries, ref 1. [d] See Table 2 for the radical's formula. [e] First coupling of PPH_2 refers to the phosphinidene P, the second coupling to the phosphino P.

experimental data are available, the DFT splitting is about −60 G, while the UMP2//UHF value is only −22.7 G.

PO_2Cl_2, $POCl_3^-$, $PFSCl_2^-$, and PO_3F^-. For PO_2Cl_2, we have obtained good agreement with the experimental results, and considerably better than the UMP2//UHF predicted splitting. For PO_3F^-, both DFT and UMP2//UHF models nicely reproduce the experimental value. While PO_2Cl_2 and PO_3F^- show small and negative hfcc's, $POCl_3^-$ and $PFSCl_2^-$ have rather large and positive splittings. For $POCl_3^-$, an overall reasonable agreement with experiment is reached by both the DFT and UMP2//UHF models. A considerable geometry influence is seen again, except for $PFSCl_2^-$ where the hfcc is less geometry dependent.

Phosphinidenes: PH, PCH_3, PNH_2, PPH_2, POH, and PSH. From the six triplet phosphinidenes considered here, only the hfcc of PH is experimentally known. This hyperfine splitting is well reproduced by all DFT methods, except when using the IGLO-III basis set. This trend also holds for other phosphinidenes; namely, the IGLO-III basis systematically yields a value considerably smaller than the corresponding TZVP, TZVP′, and TZVP″ results. The ^{31}P hfcc's of all phosphinidenes considered are similar in magnitude. The large difference in the hyperfine splittings of both P atoms in PPH_2 indicate that the unpaired electrons are mainly located on the phosphinidene P.

Isotropic Hyperfine Coupling Constants of Other Nuclei. The hfcc's of other nuclei have also been calculated. In general, a discussion of the DFT values is similar to that given for P. These values will not be reported here, but they will be included in the error analysis discussed in the following sections.

Statistical Data Analysis. Tables 5 and 6 show the mean absolute deviations from experimental values (MAD) and regression analysis for values obtained by various computational models under consideration. While Table 5 contains the values when the whole data set of 48 experimental hfcc's of P and other nuclei is taken into account, Table 6 shows the analysis for the subset of ^{31}P hfcc's only. In addition, Table 5 also contains three additional schemes which have been used by Cramer and Lim: MP2//UHF,[1] B3LYP//UHF,[2] and UMP2//UMP2. Within each subsection of Tables 5 and 6, the best MAD is displayed in bold face.

It is obvious that for the complete data set, the TZVP″ basis set yields the optimum performance in all cases. The TZVP″ set performs only slightly better than TZVP′, but considerably better than TZVP. When using DFT-optimized geometries (B3LYP and B3PW91), the B3PW91 functional performs best. However, when UMP2 geometries are employed, it turns out that the B3LYP method gives the most accurate results. An important point to note—as we emphasized in our previous work[5]—is that B3LYP//UMP2 yields better results than B3LYP as evidenced by the MAD of 15.6 and 21.8 G, respectively.

A comparison with the results obtained by Cramer and Lim for the subset of 25 radicals, reveals some interesting properties. It is seen that B3LYP/6-311G(d,p) results, obtained with UMP2 geometries, are much superior than when UHF geometries are used (MADs of 32.9 and 22.9 G, respectively). This clearly demonstrates the quality of UMP2 geometries over UHF geometries. However, it is also seen that Cramer's UMP2//

TABLE 5: Error and Regression Analysis of the Calculated hfcc's Relative to Experimental Values (G)

geometry	hfs calculation	MAD, all hfcc's (48)[a]	slope	intercept	correlation constant
B3LYP/6-311G(d,p)	B3LYP/6-311G(d,p)	28.4	1.021	−18.6	0.9961
	B3LYP/TZVP	23.4	0.971	−6.4	0.9964
	B3LYP/TZVP′	22.6	1.003	−7.8	0.9964
	B3LYP/TZVP″	**21.8**	1.003	−6.9	0.9964
	B3LYP/IGLO-III	28.0	1.045	−15.0	0.9962
	B3LYP/cc-pVTZ	25.1	0.963	−9.7	0.9973
B3PW91/6-311G(d,p)	B3PW91/6-311G(d,p)	28.1	1.011	−21.9	0.9971
	B3PW91/TZVP	22.5	0.968	−10.2	0.9979
	B3PW91/TZVP′	19.8	1.000	−11.6	0.9979
	B3PW91/TZVP″	**19.1**	1.000	−10.8	0.9979
	B3PW91/IGLO-III	23.0	1.032	−17.4	0.9978
	B3PW91/cc-pVTZ	27.6	0.954	−12.8	0.9980
MP2/6-31G(d,p)	B3LYP/6-311G(d,p)	22.9	1.023	−19.1	0.9978
	B3LYP/TZVP	18.4	0.972	−6.8	0.9985
	B3LYP/TZVP′	15.8	1.004	−8.1	0.9985
	B3LYP/TZVP″	**15.6**	1.005	−7.3	0.9985
	B3LYP/IGLO-III	18.2	1.044	−14.7	0.9983
	B3LYP/cc-pVTZ	24.6	0.961	−9.8	0.9983
MP2/6-31G(d,p)	B3PW91/6-311G(d,p)	27.1	1.006	−21.9	0.9977
	B3PW91/TZVP	21.3	0.963	−10.1	0.9986
	B3PW91/TZVP′	17.9	0.995	−11.5	0.9986
	B3PW91/TZVP″	**17.2**	0.995	−10.7	0.9986
	B3PW91/IGLO-III	19.1	1.025	−17.2	0.9982
	B3PW91/cc-pVTZ	29.8	0.947	−12.7	0.9981
UHF/6-31G(d,p)	UMP2/6-311G(d,p)[b]	16.5	1.022	3.9	0.9986
	B3LYP/6-311G(d,p)[c]	32.9	1.038	12.4	0.9948
UMP2/6-31G(d,p)	UMP2/6-311G(d,p)[b]	21.1	0.960	10.0	0.9959

[a] Number of experimental values considered is 48, including not only values for ^{31}P but also values for other nuclei. [b] Values obtained by Cramer and Lim[1] for the subset of 25 radicals. [c] Values obtained by Cramer and Lim[2] for the subset of 25 radicals.

TABLE 6: Error and Regression Analysis of Calculated ^{31}P hfcc's Relative to Experimental Values

geometry	hfs calculation	MAD, P hfcc's (24)[a]	slope	intercept	correlation constant
B3LYP/6-311G(d,p)	B3LYP/6-311G(d,p)	37.2	1.028	−20.6	0.9959
	B3LYP/TZVP	35.3	0.971	−5.9	0.9954
	B3LYP/TZVP′	33.5	1.003	−6.2	0.9954
	B3LYP/TZVP″	33.5	1.003	−6.2	0.9954
	B3LYP/IGLO-III	36.9	1.050	−15.5	0.9964
	B3LYP/cc-pVTZ	**31.9**	0.963	−4.9	0.9971
B3PW91/6-311G(d,p)	B3PW91/6-311G(d,p)	35.0	1.020	−27.1	0.9973
	B3PW91/TZVP	32.1	0.971	−12.3	0.9975
	B3PW91/TZVP′	**26.8**	1.003	−12.7	0.9975
	B3PW91/TZVP″	**26.8**	1.003	−12.7	0.9975
	B3PW91/IGLO-III	30.3	1.038	−21.1	0.9978
	B3PW91/cc-pVTZ	34.9	0.955	−10.4	0.9981
MP2/6-31G(d,p)	B3LYP/6-311G(d,p)	28.7	1.032	−25.3	0.9979
	B3LYP/TZVP	28.7	0.974	−9.9	0.9982
	B3LYP/TZVP′	**23.7**	1.007	−10.2	0.9982
	B3LYP/TZVP″	**23.7**	1.007	−10.2	0.9981
	B3LYP/IGLO-III	25.3	1.050	−19.3	0.9982
	B3LYP/cc-pVTZ	33.1	0.962	−8.5	0.9982
MP2/6-31G(d,p)	B3PW91/6-311G(d,p)	34.2	1.017	−29.8	0.9979
	B3PW91/TZVP	31.3	0.967	−14.1	0.9984
	B3PW91/TZVP′	24.6	0.999	−14.5	0.9984
	B3PW91/TZVP″	24.7	0.999	−14.7	0.9984
	B3PW91/IGLO-III	**23.8**	1.032	−22.4	0.9982
	B3PW91/cc-pVTZ	40.0	0.949	−12.2	0.9981

[a] Number of values considered is 24, i.e., the experimentally available ^{31}P hfcc's considered in this study.

UHF model performs much better than UMP2//UMP2 and nearly as well as our B3LYP//UMP2 model. As the latter two use superior geometries, a particular cancelation of errors in the UMP2//UHF model has to be present.

When we consider only the ^{31}P hfcc's in the statistical analysis, of course both TZVP′ and TZVP″ perform equally good. Essentially, the same conclusion also holds for this data subset; that is, B3LYP//UMP2 yields an optimal performance making use of the TZVP-type basis sets.

However, mean absolute deviations from experimental data may not be the right indicator to probe the accuracy of this type of calculations. Because the phosphorus hfcc's span a large range from −44.3 up to 1617.0 G, the MAD looses much of its meaning. A better way to evaluate the accuracy might be the use of linear regression. This analysis is also shown in Tables 5 and 6. For the entire data set, correlation coefficients are always better than 0.9961, and in general, best correlation is found when using UMP2 geometries. Whithin the models using UMP2 geometries, the best slopes are found for B3LYP//UMP2 using TZVP′ and TZVP″ basis sets (1.004 and 1.005, respectively) and for B3PW91//UMP2 using TZVP′ and TZVP″ basis sets (0.995). As the correlation coefficients (0.9985 and 0.9986 for B3LYP//MP2 and B3PW91//MP2, respectively) and slopes for these two models are nearly equal, the intercept is another

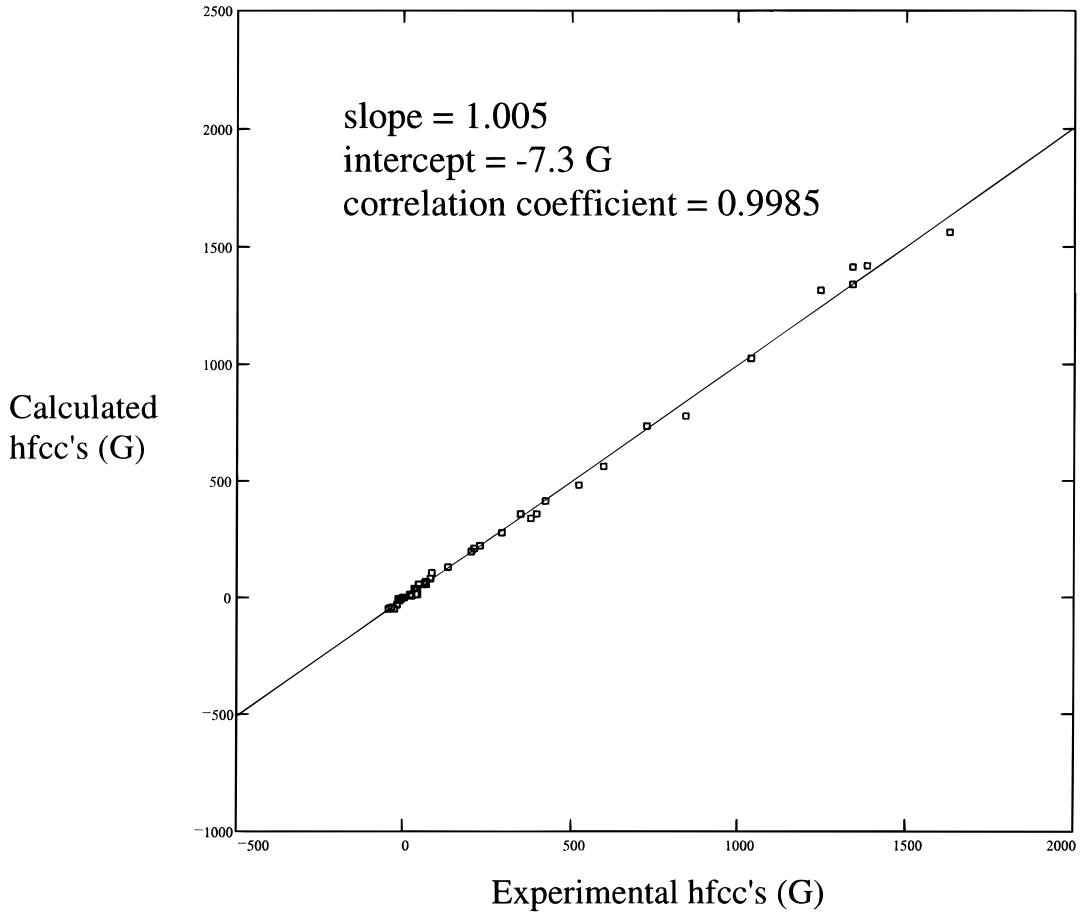

Figure 1. Regression analysis for the isotropic hyperfine splitting constants obtained by the B3LYP//MP2 method using the TZVP″ basis set. A total of 48 experimental hfcc's are included.

feature to assess the accuracy. Hence, it turns out again that the B3LYP//MP2 method using the TZVP″ basis set performs best. Note that the UMP2//UHF scheme performs nearly equal to the B3LYP/TZVP″//UMP2 model as far as slope and correlation constant are concerned. Their intercepts, however, differ by 11.2 G (3.9 and −7.3 G respectively). For the subset of ^{31}P hfcc's only (Table 6), both B3LYP//UMP2 and B3PW91//UMP2 methods yield similar results.

The overall best performance should be attributed to the B3LYP//UMP2 model using the TZVP″ basis set. A graphical representation of the regression analysis obtained with this method for the whole data set is shown in Figure 1.

Concluding Remarks

In summary, we have calculated the isotropic hyperfine coupling constants of the phosphorus nuclei in a variety of environments, using density functional theory. DFT may yield results in reasonable agreement with experiment, provided that sufficiently accurate geometries and appropriate basis sets are used. On the one hand, the best performance of DFT is attained when UMP2/6-31G(d,p)-optimized geometries are used instead of either B3LYP/6-311G(d,p) or B3PW91/6-311G(d,p)-derived geometries. On the other hand, the overall best performance is provided by the B3LYP//UMP2 method using the TZVP″ basis. A major inconvenience of the latter model is the higher computing cost in UMP2 geometry optimizations and the unavoidable problems of spin contamination. We have also compared the DFT results to the MO ones reported earlier using the UMP2/6-31G(d,p) spin densities at the UHF/6-31G(d,p) geometries. It turns out that both methods often behave differently in different cases, probably due to different types of intrinsic errors. It should be stressed that, when using UMP2 geometries instead of DFT geometries, a considerable better performance of the DFT methods comes out. In contrast, when UMP2 spin densities are used, replacement of UHF geometries by UMP2 geometries yields paradoxally much worse results. This demonstrates that the performance of an approach at an intermediate level of theory in computing spin densities results more likely from a cancelation of different errors than from an intrinsic quality of that method. Needless to say that a main factor is that gaussian functions, by definition, do not properly describe the core regions. Such a combination of method/basis set/geometry is obviously quite subtle for a full understanding and any practical proposition contains inevitably a certain ratio of empirism!

Overall, it can be concluded that, when possible, the B3LYP//UMP2 in conjunction with the TZVP″ basis set is the model of choice; otherwise, the B3LYP model is the general solution. The latter and the UMP2//UHF model proposed by Cramer and Lim perform equally well for the set of radicals considered, as some serious uncertainty for some experimental data remains and as the choice of experimental data (when different values can be found in the literature) has also a large effect on the apparent performance of a model. A greater advantage of the DFT alternative resides in its lower computational cost and the fact that it can be generalized to any type of radicals having multiple open shells, irrespective of the degree of spin contamination present in UHF(MO) wavefunctions.

Acknowledgment. The authors wish to thank the Fonds voor Wetenschappelijk Onderzoek (FWO) and the KU-Leuven Research Council (Geconcerteerde Onderzoeksacties) for continuing support.

Supporting Information Available: One figure containing the UMP2- and DFT-optimized geometries of all species considered (3 pages). Ordering information is given on any current masthead page.

References and Notes

(1) Cramer, C. J.; Lim, M. H. *J. Phys. Chem.* **1994**, *98*, 5024.

(2) Lim, M. H.; Worthington, S. E.; Dulles, F. J.; Cramer, C. J. In Chemical Applications of Density Functional Theory; Laird, B. B., Ross, R. B., Ziegler, T., Eds.; ACS Symposium Series 629; American Chemical Society: Washington, DC, 1996.

(3) Eriksson, L. A.; Malkin, V. G.; Malkina, O. L.; Salahub, D. R. *J. Chem. Phys.* **1993**, *99*, 9756.

(4) Barone, V. In Recent Advances in Density Functional Methods; Chong, D. P., Ed.; World Scientific: Singapore, 1996.; Vol. 1.

(5) Nguyen, M. T.; Creve, S.; Eriksson, L. A.; Vanquickenborne, L. G. *Mol. Phys*. **1997**, in press.

(6) Becke, A. D. *J. Chem. Phys.* **1993**, *98*, 5648.

(7) Lee, C.; Yang, W.; Parr, R. G. *Phys. Rev. B* **1988**, *37*, 785.

(8) Perdew, J. P.; Wang, Y. *Phys. Rev. B* **1992**, *45*, 13244.

(9) Godbout, N.; Salahub, D. R.; Andzelm, J.; Wimmer, E. *Can. J. Chem*. **1992**, *70*, 560.

(10) Kutzelnigg, W.; Fleischer, U.; Schindler, M. In *NMR: Basic Principles and Progress*; Springer-Verlag: Berlin, 1990; Vol. 23, 165.

(11) Woon, D. E.; Dunning, T. H., Jr. *J. Chem. Phys.* **1993**, *98*, 1358.

(12) Frisch, M. J.; Trucks, G. W.; Schlegel, H. B.; Gill, P. M. W.; Johnson, B. G.; Wong, M. W.; Foresman, J. B.; Robb, M. A.; Head-Gordon, M.; Replogle, E. S.; Gomperts, R.; Andres, J. L.; Raghavachari, K.; Binkley, J. S.; Gonzalez, C.; Martin, R. L.; Fox, D. J.; Defrees, D. J.; Baker, J.; Stewart, J. J. P.; Pople, J. A. *GAUSSIAN 94*, Revision C.3; Gaussian, Inc.: Pittsburgh, 1995.

(13) Ma, B.; Lii, J.-H.; Schaefer, H. F., III; Allinger, N. L. *J. Phys. Chem.* **1996**, *100*, 8763.

(14) Nguyen, M. T.; Ha, T. K. *Chem. Phys.* **1989**, *131*, 245.

(15) De Waal, B. F. M.; Aagaard, O. M.; Janssen, R. A. J. *J. Am. Chem. Soc.* **1991**, *113*, 9471.

(16) Knight, L. B., Jr.; Tyler, D. J.; Kudelko, P.; Lyon, J. B.; McKinley, A. J. *J. Chem. Phys.* **1993**, *99*, 7384.

(17) Begum, A.; Symons, M. C. R. *J. Chem. Soc., Faraday Trans. 2* **1973**, *m69*, 43.

(18) Aagaard, O. M.; Waal, B. F. M. D.; Cabbolet, M. J. T. F.; Janssen, R. A. J. *J. Phys. Chem.* **1992**, *96*, 614.

(19) Davies, P. B.; Russel, D. K.; Thrush, B. A. *Chem. Phys. Lett.* **1979**, *44*, 421.

(20) Nelson, W.; Jackel, G.; Gordy, W. *J. Chem. Phys.* **1970**, *52*, 4572.

(21) Bonazzola, L.; Michaut, J. P.; Roncin, J. *J. Chem. Phys.* **1981**, *75*, 4829.

(22) Colussi, A. J.; Morton, J. R.; Preston, K. F. *J. Chem. Phys.* **1975**, *62*, 2004.

(23) Mishra, S. P.; Symons, M. C. R. *J. Chem. Soc., Dalton Trans.* **1976**, 139.

(24) Colussi, A. J.; Morton, J. R.; Preston, K. F. *J. Phys. Chem.* **1975**, *79* (17), 1855.

(25) Boate, A. R.; Colussi, A. J.; Morton, J. R.; Preston, K. F. *Chem. Phys. Lett.* **1976**, *37*, 135.

(26) Serway, R. A.; Marshall, S. A. *J. Chem. Phys.* **1966**, *45*, 4098.

(27) Picone, R. F.; Raynor, J. B.; Ward, T. C. *J. Chem. Soc., Dalton Trans.* **1977**, 392.

(28) McMillan, J. A.; Clemens, J. M. *J. Chem. Phys.* **1978**, *68*, 3627.

(29) Begum, A.; Symons, M. C. R. *J. Chem. Soc. A* **1971**, 2065.

(30) Begum, A.; Subramanian, S.; Symons, M. C. R. *J. Chem. Soc. A* **1970**, 1323.

(31) Davies, P. B.; Russel, D. K.; Smith, D. R.; Thrush, B. A. *Can. J. Phys.* **1979**, *57*, 522.